Prabha Materials Science Letters
Vol. 5, No. 2, 308-322, 2026
https://doi.org/10.33889/PMSL.2026.5.2.017

Ixora Chinesis Leaf Extract Mediated Mesoporous NiO Nanoparticles for Simultaneous Catalytic Reduction of 4-Nitrophenol and Antimicrobial Resistance

S. Narayana Vavilapalli
Department of Chemistry,
Andhra University, 530003, Visakhapatnam, Andhra Pradesh, India.
&
Government Degree College, 535002, Vizianagaram Town, Andhra Pradesh, India.
E-mail: vsnchem@gcrjy.ac.in

Santi Shobha Rani
Regional Joint Director of Collegiate Education,
Zone 1&2, 533101, Rajamahendravaram, Andhra Pradesh, India.
E-mail: santikavi3@gmail.com

Gopi Mamidi
Department of Chemistry,
Dr. V. S. Krishna Government Degree College, Visakhapatnam, Andhra Pradesh, India.
E-mail: IITMGOPI@gmail.com

Sathish Mohan Botsa
Bio Enviro Chemical Solutions, 530017, Visakhapatnam, Andhra Pradesh, India.
Corresponding author: bsathish401@gmail.com

(Received on October 15, 2025; Revised on March 24, 2026 & April 13, 2026 & May 3, 2026;
Accepted on May 15, 2026)

Abstract
Water pollution caused by 4-nitrophenol (4-NP) and antibiotic-resistant pathogens presents a significant challenge for sustainable wastewater treatment. In this study, nickel oxide nanoparticles (NiO NPs) were synthesized via a green route using Ixora chinensis leaf extract and evaluated for their dual catalytic and antimicrobial performance. Structural characterization revealed crystalline NiO with an average crystallite size of 19.8 nm (XRD, Scherrer equation) and particle sizes ranging from 15-25 nm (TEM). The nanoparticles exhibited a mesoporous structure with a BET surface area of 24.6 m^2/g and a Type IV adsorption isotherm, indicating enhanced surface reactivity. The biosynthesized NiO NPs demonstrated excellent catalytic efficiency, achieving >98% reduction of 4-NP to 4-aminophenol within 35 minutes, following pseudo-first-order kinetics ($k = 0.079$ min^{-1}, $R^2 = 0.987$). Notably, the catalyst retained over 80% of its activity after 10 successive cycles, confirming excellent stability and reusability. In parallel, the nanoparticles exhibited dose-dependent antibacterial activity, with inhibition zones of 8-10 mm at 100 µg/mL against both Gram-negative (*E.coli*) and Gram-positive (*S.aureus*) strains, comparable to standard amoxicillin control. The enhanced performance is attributed to phytochemical capping agents from Ixora chinensis, which facilitate active surface sites and promote reactive oxygen species generation for microbial inactivation. These results demonstrate a sustainable nanomaterial for simultaneous pollutant degradation and pathogen control in water treatment.

Keywords- Ixora chinesis, NiO nanoparticles, Reduction of nitrophenol, Antimicrobial activity.

1. Introduction

Water contamination is a major global problem, especially from 4-nitrophenol (4-NP) and pathogenic microorganisms (Botsa et al., 2020). 4-NP, a persistent hazardous chemical found in industrial waste that

damages ecosystems and human health, perhaps leading to cancer, liver and kidney damage (Chauhan et al., 2024). Antibiotic- resistant bacteria, such as *S.aureus* and *E.coli,* cause millions of waterborne diseases every year (Gholipour et al., 2024). Traditional treatments struggle with these dual contaminants are chemical methods create byproducts while standard disinfection fails against resistant strains (Costa et al., 2026). Worse, 4-NP and microbes interact synergistically, with the chemical promoting resistant strains while organic matter shields bacteria. This complex pollution demands innovative solutions capable of addressing both contaminants simultaneously (Wang et al., 2021; Khalil et al., 2024).

The increasing of nanotechnology has sparked a lot of interest in creating multifunctional nanomaterials for antibacterial and environmental mitigations (Balto et al., 2023). Nickel oxide nanoparticles (Nio NPs) are a viable option among transition metal oxides because of their remarkable catalytic activity, chemical stability, and board spectrum antibacterial qualities (Hafeez et al., 2021).

However, the sustainability and biocompatibility of current synthesis methods are limited by the use of hazardous chemicals, high energy consumption, and intricate procedures (Sree et al., 2020). Green synthesis techniques that use plant extracts to precisely control nanoparticle morphology and surface functioning while adding bioactive capping agents have drawn attention as environmentally friendly alternatives to these constraints (Lica et al., 2018). Numerous botanical extracts, including those from *Theopuntiaficus indica*, *Leucas aspera*, *Calotropis gigantea*, *Callistemon viminalis*, *Gymnema Sylvestre*, and *Rhamnus virgata*, are used in the biogenic manufacture of NiO nanoparticles (Tailor et al., 2023).

The medicinal plant *Ixora chinensis*, which is high in terpenoids, flavonoids, and polyphenols, has lately investigated as a possible stabilizing and reducing agent for the synthesis of nanoparticles (Nadeem et al., 2025). These phytochemicals improve the catalytic and antibacterial properties of nanoparticles by functionalizing their surface and aiding in the bioreduction of $Ni2^{+}$ ions (Amin et al., 2022). Recent studies have demonstrated the efficacy of plant-mediated NiO NPs in the reduction of nitroaromatic compounds like 4-NP, a toxic byproduct of industrial waste into valuable 4-aminophenol (4-AP). Concurrently, the rise in antimicrobial resistance has necessitated the development of alternative antibacterial agents, where NiO NPs show promise due to their ability to disrupt bacterial membranes and generate reactive oxygen species.

This study reports the synthesis of NiO NPs using *Ixora chinensis* leaf extract and evaluates their dual functionality as a highly efficient catalyst for 4-NP reduction and as an antimicrobial agent against Gram-positive (*Staphylococcus aureus*) and Gram-negative (*Escherichia coli*) bacteria. In addition, the desirable nanoparticles will be characterized by UV-Vis spectrometer, SEM, EDX, TGA, XRD, TEM, FTIR, XPS, and BET analysis for studying their characteristics.

2. Experimental Section

2.1 Chemicals and Reagents

All chemicals used were of analytical grade and purchased from certified suppliers of Bio Chem Suppliers, Visakhapatnam. Double distilled water was used throughout the experiment. The following chemicals were used in this study nickel (II) sulfate ($NiSO_4$), and fresh leaves of *Ixora chinensis* were used for green synthesis.

2.2 Sample Collection and Cleaning

The fresh leaves of *Ixora chinensis* were collected in the vicinity of Andhra University, Visakhapatnam (Coordinates of the site: 17.7230928, 83.3246684) and the same was authenticated by local taxonomist

(**Figure S1**). The leaves were washed with water three times and disinfected by treating with $HgCl_2$ (0.1% w/v) and washed again. The leaves were dried in the shade under room temperature for seven days.

2.3 Preparation of Leaf Extract

The dried leaves of *Ixora chinensis* were collected and grinded into fine powder by using kitchen mixer. 2g of fine powder was weighed and transferred into 250 mL beaker and poured 100 mL water and allowed it for boiling at 70 ^oC for 1 h. Then, the mixture solution was allowed to cool to room temperature and filtered with Whatman No.1 filter paper (**Figure S2**). The filtered solution was collected in volumetric flask and sealed with aluminium foil to avoid light interactions and finally stored in refrigerator at 4 ^oC till further usage.

2.4 Green Synthesis of NiO Nanoparticles

For the synthesis of nickel oxide (NiO) nanoparticles (NPs), an aqueous 0.25 M $NiSO_4$ solution was mixed with *Ixora chinensis* leaf extract in a 1:0.75 volume ratio. The resulting mixture was continuously stirred for 10 min using a magnetic stirrer to ensure homogeneity. To facilitate the co-precipitation reaction, few drops of 0.1 M NaOH solution was added gradually in a drop wise manner to adjust the pH and promote nanoparticle formation. After heating and maintain the reaction mixture at 80^oC for 90 minutes, a dark brown precipitate appeared, indicating the generation oh NiO NPs. Centrifugation at 4,000 rpm for 15mintues was used to separate the precipitate after synthesis. To get rid of unreacted precursors and other contaminants, the recovred pellet was carefully cleaned three times using double distilled water. After being filtred, the Ixora NiO Np\Ps were dried overnight at 60^oC in a hot air oven and kept in an airtight container for future analysis and use. Furthermore, the produced Ixora-NiO NPs were shown to be insoluble in ethanol and water, but somewhat soluble in dimethyl sulfoxide (DMSO), ammonium chloride (NH_4Cl), and ammonium carbonate ($(NH_4)_2CO_3$). Based on these findings, DMSO was selected as the dispersing medium, and working solutions of NiO NPs were prepared at concentrations of 100 µg/mL, 200 µg/mL, and 500 µg/mL for antimicrobial activity evaluation.

2.5 Instrumentation

The properties of prepared NiO nanoparticles were explored by various characterization techniques. They were X-ray diffraction spectroscopy (XRD), Transmission electron microscopy (TEM), Scanning electron microscopy (SEM), UV-Vis Spectroscopy, Fourier transform infrared spectroscopy (FTIR), X-ray photoelectron spectroscopy (XPS), Thermogravimetric analysis (TGA) and Brunauer-Emmett-Teller (BET). The XRD patterns of prepared NiO NPs were measured using DX8 Bruker at a scan speed of 0.02/sec with range of 10 to 90^o. The FTIR spectrum was recorded using IR Prestige2 with the range of 500 to 4000 cm^{-1}. SEM with JEOL 6390LA system which was also equipped with energy-dispersive X-ray (EDX) spectroscopy to confirm the elemental composition. TEM using JEOL JEM-2100 operating at 200 kV. UV-Vis spectra obtained with Systronics 2200TS with wavelength scan from 200 to 800 nm. XPS analysis conducted on an Axis Ultra instrument fitted with a monochromatic Al Kα radiation source. BET by nitrogen adsorption-desorption isotherms, measured at 77 K using Quanta chrome Autosorb 1C system. TGA spectra obtained by STA8000 with temperature range of 15 °C to 1000 °C.

2.6 Catalytic Reduction of 4-Nitrophenol

The catalytic reduction of 4-nitrophenol (4-NP) into 4-aminophenol (4-AP) was employed as a model reaction to evaluate the performance of the biosynthesized NiO NPs. The reaction proceeds *via* the formation of a 4-nitrophenolate intermediate (λ_{max} = 400 nm) upon mixing 4-NP with $NaBH_4$, followed by its reduction to 4-AP (λ_{max} = 300 nm) catalyzed by the surface of NiO NPs. In an experiment, different 4-NP concentrations (3mL of 1mM) were reacted with NaBH4 (10mM) while NiO NPs (10mg) were present. Milli -Q water was used to adjust the total volume t0 5mL. Using UV-Vis spectroscopy to

measure the decline in the 400nm absorbance peak, the reaction's progress was tracked in real-time.

2.7 Evaluation of Antimicrobial Activity

The agar well diffusion method was used to evaluate the antimicrobial activity of the produced NiO NPs. 0.8g of Nutrient agar powder was dissolved in 20mL of distilled water to create the agar medium, which was then autoclaved for 20 minutes at 121°C to sterilize it. To create the bacterial suspension for bacterial injection, 100µL of *Escherichia coli (E.coli*) culture was diluted with 1mL of sterile water. To guarantee even microbial distribution, the *E.coli* suspension was evenly distributed across the surface of sterile petri plates after the sterilized agar was added and allowed to harden. Using a sterile borer, four aseptic wells were made on each plate. NiO NPs solutions at concentrations of 100µg/mL, and 500µg/mL were added to other wells; one well was used as the positive control loaded with an amoxicillin solution. The zones of inhibition were evaluated to assess the antibacterial efficiency after the plates were incubated for 48 hours at 37^0C.

3. Results and Discussion

3.1 Formation of *Ixora*-Mediated NiO NPs

NiO NPs were developed by reducing Ni^{2+} ions from mM aqueous $NiSO_4$ (1%w/v) using *Ixora chinensis* leaf extract, as seen by a noticeable shift in hue from pale blue to green. The presence of phytochemicals in the reduction process was confirmed by the absence of this change in the control (aqueous $NiS0_4$ alone) (**Table 1**). The proposed mechanism (Equations (1) to (3)) involves, electron donation by hydroxyl (O-H) and carbonyl (C=O) groups of polyphenols/flavonoids in the extract, reducing Ni^{2+} to intermediate Ni^{+} (Equation (1)). Further reduction of Ni^{+} to metallic nickel (Ni^o) by flavonoids (Equation (2)). Oxidation of Ni^o in aqueous medium, leading to the formation of stable NiO NPs (Equation (3)) (Irannanavar et al., 2026). The extract's organic components, including as proteins and polyphenols, stabilize the NPs and stop them from clumping together by acting as capping agents.

$$Ni^{2+} + Phenolic - OH \rightarrow Ni^{+} + Phenolic - O + H^{+} \quad (1)$$

$$2Ni^{+} + Flavonoid \rightarrow 2Ni^{0} + Oxidized\ flavonoid \quad (2)$$

$$2Ni^{0} + \frac{1}{2}O_2 \rightarrow NiO \quad (3)$$

Table 1. Reported green synthesis of NiO NPs using various plant extract (Hussain et al., 2023).

Plant extract	Nickel salt used for the synthesis	Applications tested
Ixora chinensis leaves (This study)	$NiSO_4$	Reduction of 4-Nitropheol, Antibacterial activity
Azadirachta indica and *Psidium guajava* leaves	$NiCl_2$	Cytotoxic effect against HT29 cell line
Camellia Sinensis leaves	$NiCl_2$	Photocatalytic activity for dye degradation
Euphorbia maculate aerial parts	$NiCl_2$ and Fe_3O_4	Dye removal efficiency
Fumaria officinalis leaves	$NiSO_4$	Anti-human ovarian cancer
Calotropis gigantea leaves	$Ni(NO_3)_2$	for antimicrobial potentials, catalytic degradation of methylene blue
Ocimum sanctum leaves	$NiNO_3$ and $NiSO_4$	Used as adsorbent hazardous anionic pollutants, dyes and antimicrobial activity against *E-coli* and pseudomonas
Phlomis cancellata Bunge	$Ni(NO_3)_2$	Photocatalytic degradation
Apium graveolens	$Ni(CH_3COO)_2$	Removing aliphatic hydrocarbons in crude oil
Medicago sativa	$Ni(NO_3)_2$	Used for bioreduction
Aegle marmelos Correa leaves	$NiCl_2$	Anti-inflammatory and larvicidal activity
Ananas comosus leaves	$NiCl_2$	Polymer industry
Hordeum vulgare seeds	$Ni(NO_3)_2$	catalytic activity for the degradation of methylene blue
Agathosma betulina leaves	$Ni(NO_3)_2$	Electrochemical storage devices
Vernonia Amygdalina leaves	$NiCl_2$	Photocatalytic degradation of organic dyes, antimicrobial activity

Table 1 continued…

Hydrangea paniculata Flower	$Ni(NO_3)_2$, and $Fe(NO_3)_2$	Microwave, electronic, storage devices, ferrofluids, catalysts
Rhamnus prinoides leaves	$NiFe_2O_4$	Gas sensing, Antibacterial activity
Acacia nilotica leaves	$Ni(NO_3)_2$	Electrochemical, Antibacterial, haemolytic

3.2 Optical Properties

The UV-Vis absorption spectrum of the NiO NPs synthesized using *Ixora chinensis* leaf extract exhibits a broad absorption band in the range of 300-400 nm, with a prominent peak centered on 348 nm as depicted in **Figure 1a**. This absorption is attributed to the interband transitions ($O^{2-} \rightarrow Ni^{2+}$ charge transfer) and the characteristic d-d transitions of Ni^{2+} ions in the octahedral crystal field of NiO (Sukumaran et al., 2025). The absence of sharp peaks suggests the formation of small, well-dispersed nanoparticles with minimal aggregation. The slight absorption tail extending into the visible region (400-800 nm), which are common in transition metal oxide nanostructures (Sree et al., 2020). The optical band gap was estimated using Tauc plot analysis (a direct band gap), and found to be 3.56 eV for prepared *Ixora*-NiO NPs.

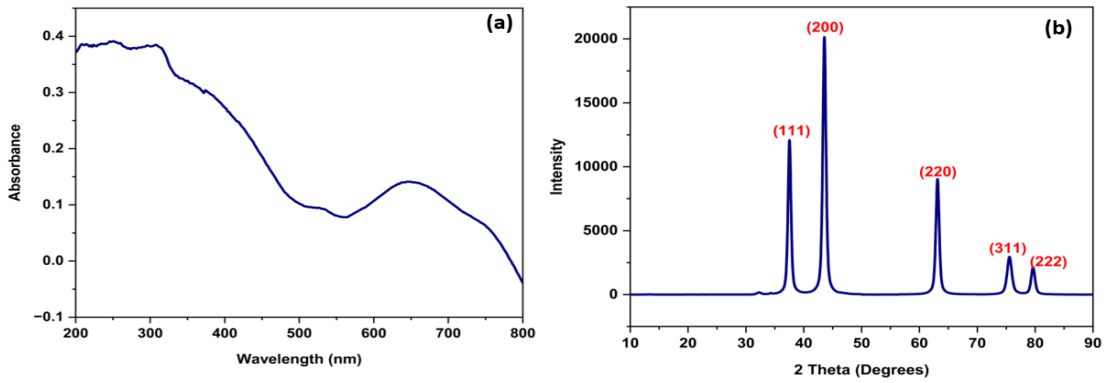

Figure 1. (a) UV-Vis absorption spectrum, and (b) XRD patterns of *Ixora*-mediated NiO NPs.

3.3 Crystal Planes and Size

The X-ray diffraction (XRD) pattern of NiO NPs synthesized using *Ixora chinensis* leaf extract exhibits distinct diffraction peaks at 2θ values of 37.6°, 43.6°, 63.2°, 75.6°, and 79.7° (**Figure 1b**), which correspond to the (111), (200), (220), (311), and (222) crystallographic planes, respectively. These peaks are characteristic of the face-centered cubic (FCC) structure of NiO (JCPDS card no. 47-1049), confirming the formation of a pure crystalline phase (Sree et al., 2020; Tailor et al., 2023). The absence of additional peaks indicates the high purity of the synthesized NiO NPs, with no detectable impurities or secondary phases. The sharp and well-defined peaks suggest good crystallinity, which is further supported by the relatively high intensity of the reflections. The use of *Ixora chinensis* leaf extract as a green reducing and stabilizing agent likely facilitated the controlled growth of NiO NPs, as evidenced by the uniform diffraction pattern. Equation (4) signifies the Debey-Scherrer's calculation for obtain the average crystalline size (D) of prepared *Ixora* mediated NiO NPs and the result is 19.8 nm.

$$S = \frac{k}{\beta \cos \theta} \tag{4}$$

3.4 Functional Moieties

The FTIR (fourier transform infrared spectroscopy) spectrum of the biosynthesized NiO NPs reveals key functional groups involved in the reduction, stabilization, and capping of the nanoparticles (**Figure 2**). O-

H stretching vibrations from residual water or phenolic hydroxyl groups in the leaf extract are responsible for the broad absorption band at 3369 cm^{-1}, whereas C=O stretching of carbonyl groups (flavonoids, terpenoids) that function as reducing agents is responsible for the peak at 1635cm^{-1}. The development of Ni-O stretching vibrations, which aretypical of crystalline NiO, is confirmed by the prominent band near 616cm^{-1} (Sree et al., 2020; Sukumaran et al., 2025). The existence of organic capping agents generated from the leaf extract of Ixora chinesis, which stabilize the NPs and prevent aggregation, is suggested by additional peaks at 1336cm^{-1} (C-N stretching of amines/proteins) and 1025cm^{-1} (C-O). The effective conversion of phytochemical during synthesis is shown by the lack of strong peaks over 3369 cm^{-1} (O-H or N-H).

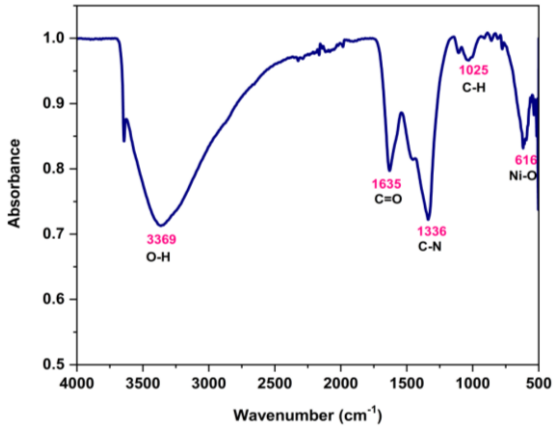

Figure 2. FTIR spectrum of synthesized *Ixora*-mediated NiO NPs.

3.5 Morphological Characterization

The morphology of NiO NPs made with *Ixora chinensis* leaf extract is shown in the scanning electron microscopy (SEM) images (**Figures 3a, 3b**). Higher magnification (50.00KX, **Figure 3b**) verifies the NPs' nanoscale dimensions (50-100 nm) and rough surface roughness, which are probably caused by organic capping agents from the extract. At 10.00 KX magnification (**Figure 3a**), the NPs appear as aggregated clusters with quasi-spherical shape. The presence of nickel (Ni) and oxygen (O) as the major elements is confirmed by the energy dispersive X-ray spectroscopy (EDX) spectrum (**Figure 3c**), which shows distinct peaks at 0.85 keV (Ni Lα) and 0.52 keV (O Kα). The Ni:O atomic ratio of 42.6:57.4, as determined by quantitative EDX analysis, is consistent with the stoichiometry of NiO, with slight variations ascribed to surface hydroxylation or residual organic matter. The absence of extraneous peaks confirms the high purity of the biosynthesized NPs.

Further, the transmission electron microscopy (TEM) images reveal well dispersed, quasi-spherical NiO NPs with an average diameter of 15-25 nm. The high-resolution TEM image (**Figure 4a, 4b**) shows distinct lattice fringes with an interplanar spacing of 0.24 nm, corresponding to the (111) plane of face-centered cubic (fcc) NiO. The nanoparticles exhibit moderate uniformity in size and shape, with some aggregation observed due to the high surface energy of the nanoparticles. The clear lattice fringes and clear particle boundaries confirmed the high crystallinity of the biosynthesized NiO NPs. The selected area electron diffraction (SAED) pattern displays concentric rings with bright spots, indicating the polycrystalline nature of the sample. The diffraction rings can be indexed to the planes of fcc NiO (JCPDS No. 47-1049), which matches perfectly with the XRD results. The sharp diffraction spots superimposed on the rings suggest the presence of some larger crystalline domains (**Figure 4c**).

The histogram analysis of 150 particles reveals a narrow size distribution ranging from 10 to 60 nm, with a maximum population at 18 nm. The distribution's Gaussian fit yields an average particle size of 34.8 nm (**Figure 4d**). Good control over particle size during the green synthesis process is indicated by the comparatively minimal standard deviation.

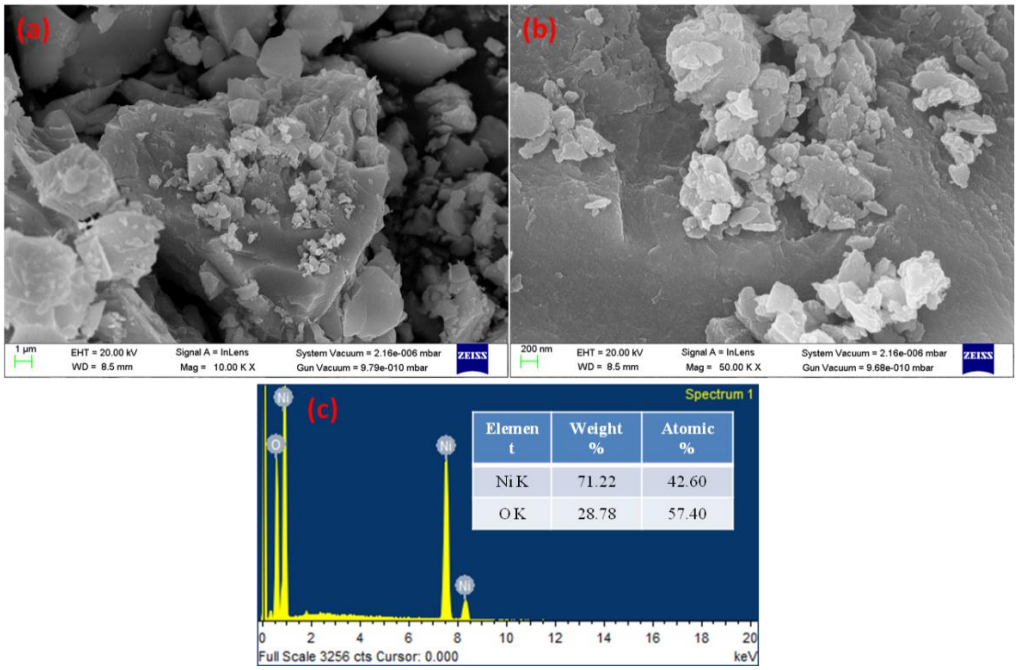

Figure 3. SEM (a, b) and EDX (c) images of biosynthesized NiO NPs.

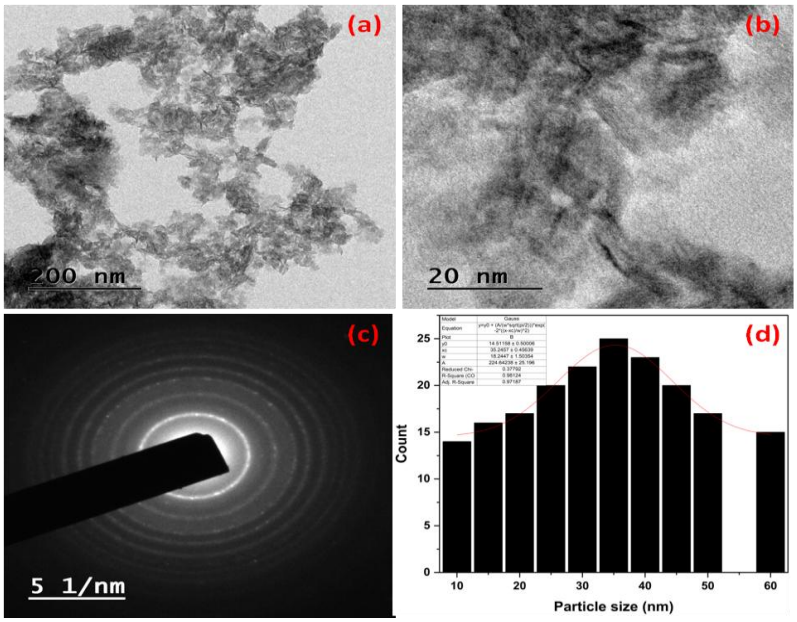

Figure 4. TEM images (a, b), SAED (c) and histogram distribution graph (d) of biosynthesized NiO NPs.

3.6 Chemical States and Surface Composition

The high-resolution XPS spectra offer comprehensive details regarding the surface composition and chemical state of the NiO NPs made with leaf extract from Ixora chinensis. **Figure 5a** shows the Ni 2p spectrum shows two main spin-orbit doublets at binding energies of 854.3 eV (Ni $2p_{3/2}$) and 871.8 eV (Ni $2p_{1/2}$), characteristic of Ni^{2+} in NiO (Sukumaran et al., 2025). The $2p_{3/2}$ and $2p_{1/2}$ peaks' energy separation of 17.5 eV is in line with typical NiO reference data. **Figure 5b** exhibits the O 1s spectrum can be deconvoluted into three components: 529.2 eV, corresponds to lattice oxygen (O^{2-}) in NiO 531.1 eV. Attributed to surface hydroxyl groups (OH^-) or oxygen vacancies 532.5 eV: Associated with adsorbed water or organic species from the plant extract.

With a small oxygen excess probably caused by surface hydroxylation, the atomic ratio of Ni: O determined from the peak regions is roughly 1:1.1, which is in good agreement with the predicted stoichiometry of NiO. The successful capping of nanoparticles by phytochemicals from the *Ixora chinensis* extract is confirmed by the presence of organic related peaks in the O 1s spectrum, which is in line with FTIR findings.

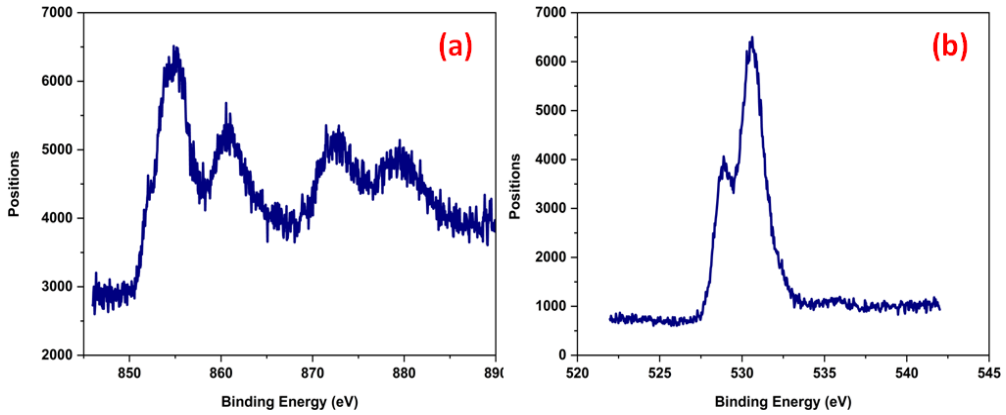

Figure 5. XPS curves with (a) Ni 2p and (b) O 1s.

3.7 Surface Area

The produced Ixora mediated NiO NPs exhibit a Type IV isotherm with a clear H3 hysteresis loop in the relative pressure range (P/Po = 0.4-0.9), which is typical of mesoporous materials with slit shaped pores, according to the Brunauer-Emmett-Teller (BET) analysis. At higher relative pressures (P/Po>0.8), The steep adsorption branch indicates the existence of interparticle porosity brought on by nanoparticle aggregation (Bonneviot et al., 2024). A high surface-to-volume ratio, which is advantageous for catalytic and adsorption application, as indicated by the predicted BET surface area of 24.6m^2/g (**Figure 6a**). The material's mesoporous nature is further supported by the average pore diameter of 0.027 cc/g and the overall pore volume. The biosynthesized Nio NPs are appropriate for use in gas sensing, catalysis, and energy storage because of their porosity nature, which improves mass transport and active site accessibility.

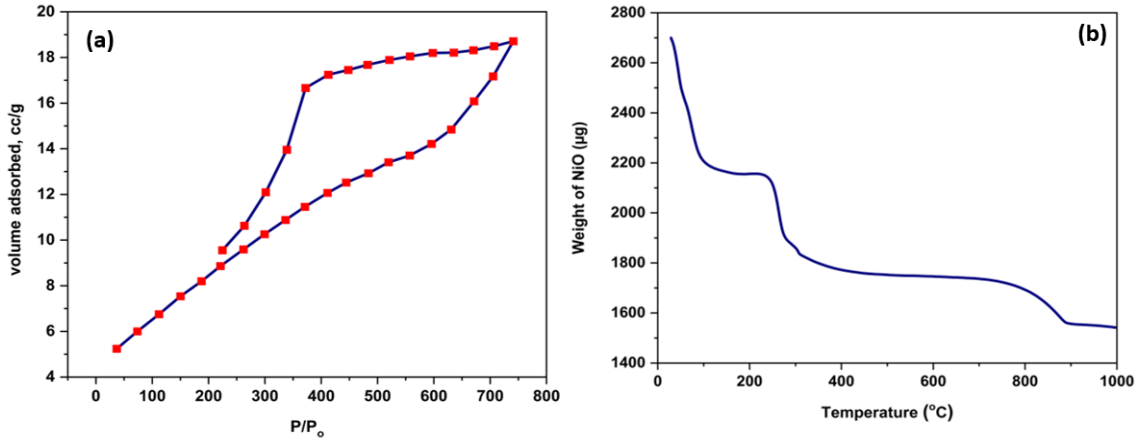

Figure 6. (a) N_2 adsorption-desorption surface assay, and (b) Thermogram curve of *Ixora*-NiO NPs.

3.8 Thermal Stability

A three-stage thermal breakdown trend is revealed by Thermogravimetric analysis (TGA) of NiO NPs mediated by *Ixora chinensis*. The evaporation of physiosorbed water and the dehydratation of surface hydroxyl groups cause an initial 7% mass loss between 30 and 200 °C (Tailor et al., 2023). The oxidation of leftover phytochemicals and the thermal degradation of organic capping agents obtained from the plant extract are responsible for the main disintegration event (17% mass loss) that takes place between 200 and 400 °C. The curve stabilizes with little mass loss (<2%) beyond 400°C, as seen in **Figure 6b**, suggesting full production of thermally stable, crystalline NiO NPs with a final residue yield of 76%. The successful synthesis of pure NiO is appropriate for high temperature applications, is confirmed by the strong thermal stability beyond 400 °C, and the total organic content of 23% indicates effective capping by biomolecules obtained from plants. The regulated breakdown profile and lack of phase transitions at high temperatures show how effective the green synthesis method is in creating thermally stable nanomaterials with distinct surface properties. The effective biosynthesis of NiO NPs and superior thermal stability is confirmed by these findings, which also show a strong correlation with the FTIR and XPS data.

3.9 Catalytic reduction Nitrophenol into Aminophenol

Ixora-Nio NPs catalyze the time-dependent reduction of 4-nitrophenolate ion (4-NP) to 4- aminophenol (4-AP), as seen by the UV-Vis spectra in **Figure 7a**. With reaction time, the distinctive 4-nitrophenolate absorption peak at 400nm gradually diminishes, and a new peak that represents the synthesis of 4-AP appears at 300nm. This isothermal spectral evolution confirms the complete conversion of 4-NP to 4-AP within 30 minutes. The unique absorbance profiles of the reactants and products are displayed in **Figure 7b**, where the decolorization of the solution and the disappearance of the yellow color (40nm peak) clearly confirm the completion of the reaction The suggested mechanism entails 4-NP and BH4- adsorption on the NiO surface, electron transfer from BH4- to 4-NP via Ni2+ redox sites, and desorption of the resultant 4-AP (Chauhan et al., 2024). The dual function of NiO NPs as electron mediators and adsorption platforms is highlighted in this approach, and their phytochemical capping probably improves reactant accessibility. The linear plot of ln (A_t/A_0) versus time in **Figure 7c** indicates pseudo first order reaction kinetics, with the slope giving the apparent rate constant (k). The kinetic model is validated by the excellent linear regression value ($R^2 = 0.987$). The conversion efficiency is quantified in **Figure 7d**, which displays >95% 4-NP decrease in 35 minutes.

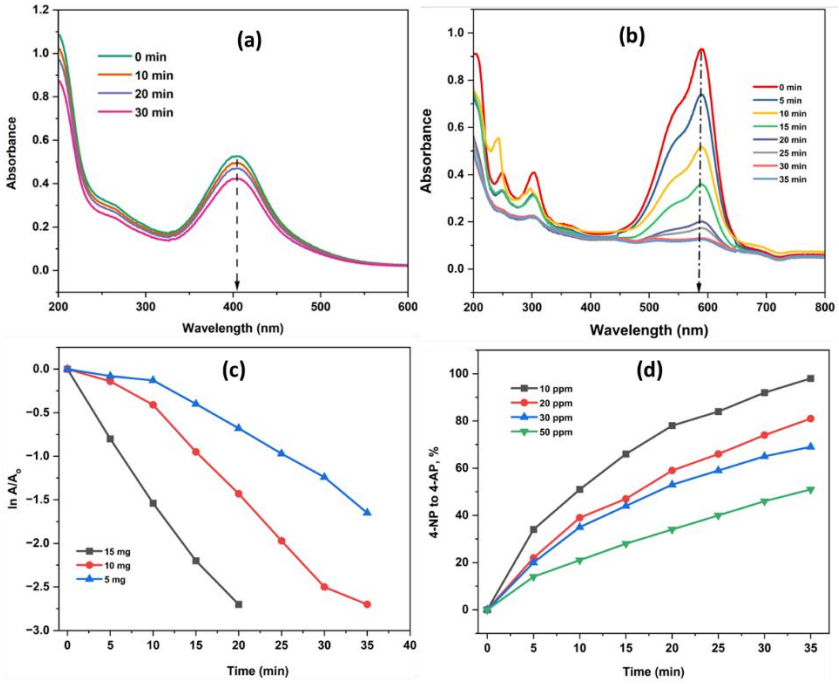

Figure 7. Reduction of 4-NP into 4-AP using biosynthesized NiO NPs (a) 4-nitrophenolate ion, (b) 4-NP reduction, (c) Catalyst loading amount and (d) effect of 4-NP concentration.

a) Reusability and Stability

Through several reaction cycles and structural analysis, the stability and catalytic reusability of the biosynthesized ixora NiO NPs were methodically assessed. The nanoparticles demonstrated outstanding reusability in the 4-nitrophenol reduction reaction, retaining over 80% conversion efficiency even after 10 consecutive cycles, as seen in **Figure 8a**. The strong structural integrity of the NiO NPs and the stabilizing effect of phytochemical capping agents made from the extract of Ixora chinensis, which successfully stop nanoparticles aggregation or active site leaching during the catalytic process, are responsible for this outstanding performance. By comparing the crystalline structure before (first run) and after (10th run) the reaction cycles, XRD analysis (**Figure 8b**) further verified the stability of the produced NiO NPs. The XRD patterns showed identical peak positions of fcc NiO, with no detectable phase changes or impurity formation. Only minimal peak broadening was observed after ten cycles, suggesting less than 2 nm change in crystallite size according to Debey-Scherrer's analysis.

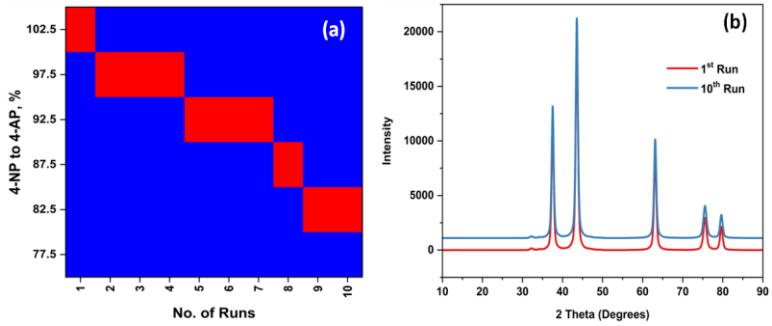

Figure 8. (a) Reusability and (b) Stability of synthesized *Ixora*-NiO NPs.

b) Plausible Mechanism

The reduction of 4-nitrophenol (4-NP) to 4-aminophenol (4-AP) using NiO nanoparticles (NiO NPs) synthesized from *Ixora chinensis* leaf extract in the presence of sodium borohydride ($NaBH_4$) proceeds through a surface-catalyzed electron transfer mechanism (Botsa et al., 2020). In an aqueous medium, $NaBH_4$ acts as a strong reducing agent, generating hydride ions (H^-), while also creating a basic environment that facilitates the deprotonation of 4-NP into its phenolate form, which absorbs strongly around 400 nm. This 4-nitrophenolate ion adsorbs onto the surface of NiO NPs due to electrostatic interactions. Simultaneously, BH_4^- ions also adsorb onto the catalyst surface. The NiO NPs, which are stabilized and capped by phytochemicals from the Ixora chinensis extract (such as flavonoids and polyphenols), facilitate the transfer of electrons from the hydride ions to the nitro group ($-NO_2$) on 4-NP.

The reduction occurs in a stepwise manner firstly (**Figure 9**), the nitro group is reduced to a nitroso intermediate, then to hydroxylamine (-NHOH), and finally to the amino group ($-NH_2$), yielding 4-aminophenol. Protons required for these reductions are provided by the aqueous environment and the decomposition of $NaBH_4$. The product 4-aminophenol desorbs from the catalyst surface when the reduction is finished, leaving the NiO NPs catalytically active for additional reaction cycles. By increasing surface activity and particle dispersion, the phytochemical components of Ixora chinensis not only support the production of NiO but also enhance catalytic efficiency.

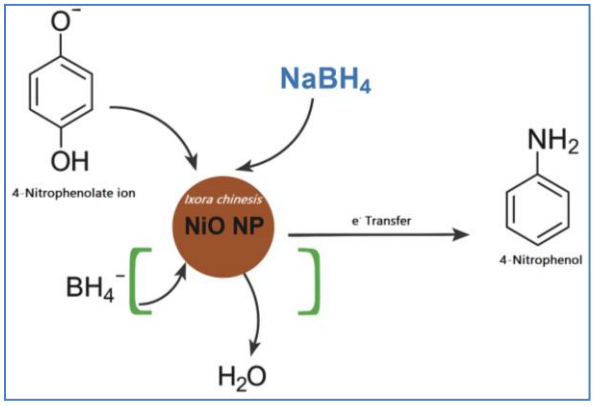

Figure 9. Plausible mechanism for reduction of 4-NP into 4-AP using NiO NPs.

3.10 Antibacterial Activity

The zone of inhibition studies showed that the biosynthesized NiO NPs exhibited strong antibacterial activity against both Gram-positive (*Staphylococcus aureus*) and Gram -negative (*Escherichia coli*) bacteria (**Table 2**). Ixora NiO NPs produced inhibitory zones of 5mm and 6mm for *S. aureus* and *E. coli*, respectively, at the lowest tested concentration (10µg/mL). With zones growing to 7mm (*Staphylococcus aureus*) and 10mm (*Escherichia coli*) at the maximum dosage of 100µg/mL, the antibacterial action demonstrated a definite dose-dependent response. Although these finding are encouraging, the activity was slightly less than that of the positive control amoxicillin (14mm for both strains), as seen in **Figure 10**.

The release of Ni_2^+ ions, which damage microbial cell membranes and produce reactive oxygen species, the nanoparticles direct physical interaction with bacterial cell walls, which results in structural damage, and possible synergistic effects from phytochemicals capping the NiO NPs are a likely contributing factor to the observed antibacterial mechanism (Sree et al., 2020). Gram negative bacteria may be more

vulnerable to nanoparticle penetration because of the makeup of their outer membrane, which could explain the activity against *E. coli* compared to *S. aureus* at higher concentrations (Tailor et al., 2023).

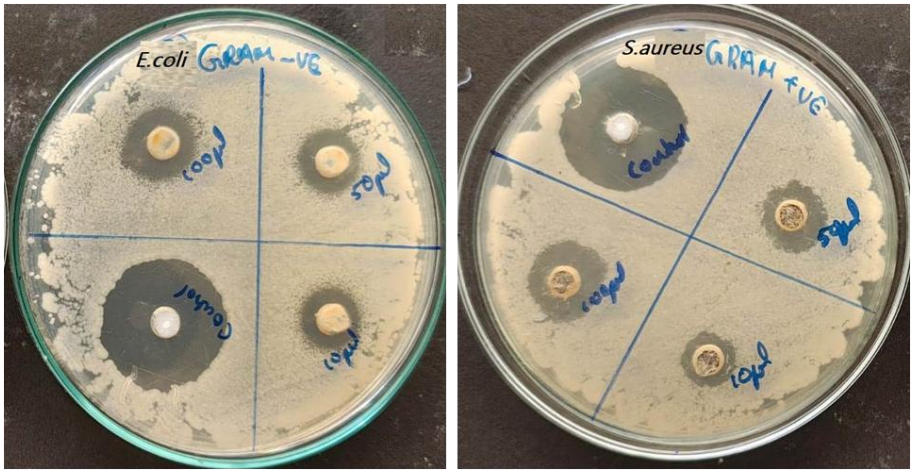

Figure 10. Antibacterial activity of biosynthesized NiO NPs over *E.coli* and *S.aureus*.

Table 2. Antibacterial performance of *Ixora*-mediated NiO NPs.

Test compound	Zone of Inhibition (mm)	
	S.aureus	***E.coli***
10 µg/mL	5	6
50 µg/mL	7	8
100 µg/mL	8	10
Amoxicillin	14	14

4. Conclusions

The dual functionality of the *Ixora chinensis* mediated NiO NPs created in this study successfully addresses two important water contamination issues. Because of their ideal size, crystallinity, and phytochemical stability, the biosynthesized NiO nanoparticles demonstrated higher 4-NP reduction efficiency and recyclability as a catalyst when compared to numerous documented green produced NiO NPs. Their strong antibacterial action against resistant strains shows promise in the fight against aquatic infections in situations where traditional therapies are ineffective. Compared to chemical approaches, the green synthesis methodology produces NiO NPs with improved performance characteristics while also offering environmental benefits. Although more study is required to improve large-scale production and evaluate long-term environmental implications, this work offers a platform for creating multifunctional nanomaterials that can simultaneously address chemical and biological pollutants in waste water systems. The results make plants synthesised Nio NPs attractive options for environmentally friendly water treatment methods.

Conflicts of Interest

No conflicts of interest.

Acknowledgments

Not applicable.

AI Disclosure

During the preparation of this work the author(s) used generative AI in order to improve the language of the article. After using this tool/service, the author(s) reviewed and edited the content as needed and take(s) full responsibility for the content of the publication.

Supporting Information

Figure S1. *Ixora chinesis* plant.

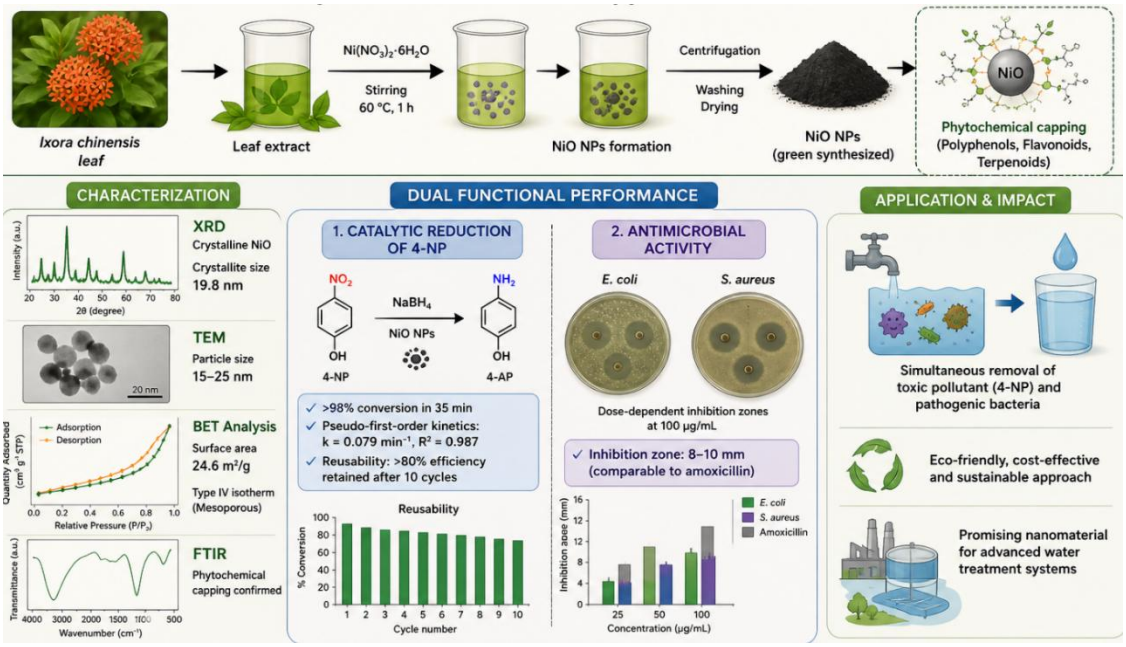

Figure S2. Schematic representation on NiO NPs using *Ixora* leaf extract.

References

Amin, S., Sher, M., Ali, A., Rehman, M.F., Hayat, A., Ikram, M., Abbas, A., & Amin, H.M.A. (2022). Sulfonamide-functionalized silver nanoparticles as an analytical nanoprobe for selective Ni (II) sensing with synergistic antimicrobial activity. *Environmental Nanotechnology, Monitoring & Management, 18,* 100735. https://doi.org/10.1016/j.enmm.2022.100735

Balto, H., Amina, M., Bhat, R.S., Al-Yousef, H.M., Auda, S.H., & Elansary, A. (2023) Green synthesis of nickel nanoparticles using salvadora persica and their application in antimicrobial activity against oral microbes. *Microbiology Research, 14*(4), 1879-1893. https://doi.org/10.3390/microbiolres14040128

Bonneviot, L., Albela, B., Gao, F., Perriat, P., Epicier, T., & El Eter, M. (2024). Protocrystallinity of monodispersed ultra-small templated mesoporous silica nanoparticles. *Nanomaterials, 14*(12), 1052. https://doi.org/10.3390/nano14121052

Botsa, S.M., Kumar, Y.P., & Basavaiah, K. (2020). Facile simultaneous synthesis of tetraaniline nanostructures/silver nanoparticles as heterogeneous catalyst for the efficient catalytic reduction of 4-nitrophenol to 4-aminophenol. *RSC Advances*, *10*, 22043-22053. https://doi.org/10.1039/D0RA03327H

Chauhan, G., Chauhan, S., Soni, S., Kumar, A., Negi, D.S., & Bahadur, I. (2024). Catalytic reduction of 4-nitrophenol using synthesized and characterized CoS@MorphcdtH/CoS@4-MPipzcdtH nanoparticles. *Journal of the Chinese Chemical Society, 70*(4), 879-893. https://doi.org/10.1002/jccs.202200459

Costa, M., Terrón, D., Leal, C., Pazos, M., Sanromán, Á., Ferreira, E.C., & Quintelas, C. (2026). Disinfection in wastewater treatment: from conventional to emerging technologies. *Journal of Water Process Engineering, 87*, 110070. https://doi.org/10.1016/j.jwpe.2026.110070

Gholipour, S., Nikaeen, M., Mohammadi, F., & Rabbani, D. (2024). Antibiotic resistance pattern of waterborne causative agents of healthcare-associated infections: a call for biofilm control in hospital water systems. *Journal of Infection and Public Health, 17*(7), 102469. https://doi.org/10.1016/j.jiph.2024.102469

Hafeez, M., Shaheen, R., Akram, B., Ahmed, M.N., ul-Abdin, Z., Haq, S., Din, S.U., Zeb, M., & Khan, M.A. (2021). Green synthesis of nickel oxide nanoparticles using Populus ciliata leaves extract and their potential antibacterial applications. *South African Journal of Chemistry, 75*(1), 168-173. https://doi.org/10.17159/0379-4350/2021/v75a21

Hussain, S., Muazzam, M.A., Ahmed, M., Ahmad, M., Mustafa, Z., Murtaza, S., & Imran, M. (2023). Green synthesis of nickel oxide nanoparticles using Acacia nilotica leaf extracts and investigation of their electrochemical and biological properties. *Journal of Taibah University for Science, 17*(1), 2170162. https://doi.org/10.1080/16583655.2023.2170162

Irannanavar, K.M., Gaddigal, A.T., Shivappa, P., Mirjankar, M.R., Poojari, P.B., Huyilagola, P.V., & Kamanavalli, C.M. (2026). Biosynthesis of nickel oxide nanoparticles using ethnomedicinal plant Crotalaria pallida leaves extract: evaluation of antibacterial, antioxidant, antiangiogenic, cytotoxicity and ROS expression against HCT-116 and PANC-1 cells. *Next Nanotechnology, 9*, 100385. https://doi.org/10.1016/j.nxnano.2026.100385

Khalil, M.T., Zhang, P., Han, G., Wu, X., Li, B., & Xiao, M. (2024). Green synthesis of gold nanoparticles for catalytic reduction of 4-nitrophenol and methylene blue for sustainable development. *Sustainable Polymer & Energy*, *2*(1), 10002. https://doi.org/10.35534/spe.2024.10002

Lica, I.C.L., dos Santos Soares, A.M., de Mesquita, L.S.S., & Malik, S. (2018). Biological properties and pharmacological potential of plant exudates. *Food Research International, 105*, 1039-1053. https://doi.org/10.1016/j.foodres.2017.11.051

Nadeem, R., Imran, M., Saeed, Z., Pervaiz, M., & Younas, U. (2025). Exploring the therapeutic potential of *Ixora* extract: a comprehensive review of mediated studies. *Advances in Traditional Medicine, 25*(1), 107-144. https://doi.org/10.1007/s13596-024-00797-4

Sree, G.S., Botsa, S.M., Reddy, B.J.M., Ranjitha, & K.V.B. (2020). Enhanced UV-Visible triggered photocatalytic degradation of Brilliant green by reduced graphene oxide based NiO and CuO ternary nanocomposite and their antimicrobial activity. *Arabian Journal of Chemistry, 13*(4), 5137-5150. https://doi.org/10.1016/j.arabjc.2020.02.012

Sukumaran, J., Priya, M., Venkatesan, R., Sathiasivan, K., Khan, M.R., & Kim, S.-C. (2025). Green synthesis of nickel oxide nanoparticles using leaf extract of *Aegle marmelos* and their antibacterial, anti-oxidant, and in vitro cytotoxicity activity. *Microscopy Research and Technique, 88*(10), 2830-2842. https://doi.org/10.1002/jemt.70054

Tailor, G., Chaudhary, J., Jandu, S., Chetna, Mehta, C., Yadav, M., & Verma, D. (2023). A review on green route synthesized nickel nanoparticles: biological and photo-catalytic applications. *Results in Chemistry, 6,* 101195. https://doi.org/10.1016/j.rechem.2023.101195

Wang, Y.-L., Dai, Y.-M., & Tsai, M.-H. (2021) Highly efficient and recyclable Fe_3C/Au@NG catalyst for 4-nitrophenol reduction. *Catalysis Communications, 149,* 106251. https://doi.org/10.1016/j.catcom.2020.106251